10.1098/rspa.2001.0871

THE ROYAL SOCIETY

Trapping of water waves by pairs of submerged cylinders

By R. Porter

School of Mathematics, University of Bristol, Bristol BS8 1TW, UK

Received 30 November 2000; accepted 16 July 2001; published online 24 January 2002

This paper provides strong numerical evidence for the existence of two-dimensional trapped waves supported by a symmetrically arranged pair of submerged cylinders with a particular form of cross-section. Wide-spacing arguments applied to single submerged obstacles exhibiting zeros of transmission are used as the basis for seeking trapped waves. The integral equation technique developed for the scattering by arbitrary submerged obstacles in Porter (2001) is extended for this problem, and it is shown how trapped waves correspond to the point of intersection of two independently computed curves. Results are given for a variety of symmetrical pairs of submerged obstacles.

Keywords: trapped waves; submerged cylinders; arbitrary cross-section; two-dimensional flow

1. Introduction

Trapped water waves in two-dimensional linearized flows were first discovered by McIver (1996), who constructed a solution in which localized time-harmonic fluid oscillations were proved to exist in the presence of two partly immersed bodies, each belonging to a family of cross-sections. These oscillations are called trapped waves, since they persist for all time in the vicinity of the trapping structure without radiating any of their energy away from the structure to infinity. As a consequence, they therefore also represent a non-uniqueness in a corresponding forcing problem, such as the scattering of waves by such structures.

The existence of trapped waves in certain three-dimensional wave problems involving finite periodicity in one of the horizontal directions is well established (see Evans & Kuznetsov (1997) for an extensive review). This is because trapped waves for this type of three-dimensional problem usually occur at frequencies lying below a 'cut-off' frequency, which ensures that a wave motion local to a trapping structure (if one can be found satisfying other conditions of the problem) is certain to remain localized for all time. However, in general no such cut-off exists for the two-dimensional water wave problem and hence the task of finding trapped waves in this case is extremely challenging.

McIver's (1996) example used a so-called inverse procedure, by placing a source and a sink of equal strength in the free surface of a fluid of infinite depth at a separation such that the waves generated by the source–sink pair cancels at either infinity. Any pair of streamlines of the resulting flow which isolate the two singularities can be interpreted as the boundaries of solid surface-piercing bodies and the fluid motion exterior to these bodies as trapped waves. This inverse procedure has since been used to provide further examples of two-dimensional trapped waves. Its advantage is clear: in the construction of a prospective trapped-wave solution one automatically ensures that the far-field vanishes, as is required. Its disadvantage is that the shape of a trapping structure, if a suitable candidate can be found, cannot be selected *a priori*.

More recently, McIver (2000) has provided an example of wave trapping by a specific pair of submerged cylinders using the inverse procedure with a combination of submerged vertical and horizontal dipoles. However, the cylinders are only submerged to a very small depth below the free surface. So far this is the only example of a trapping structure that is entirely submerged. It is therefore interesting and mathematically challenging to seek further examples of pairs of submerged cylinders that can trap waves. There are limitations on the geometries that can be considered, since Simon & Ursell (1984) proved that two-dimensional submerged obstacles in deep water cannot support trapped waves if entirely contained between two lines drawn at angles of 45° to the vertical from a single point on the free surface. In fluid of finite depth, this angle is increased slightly to $45\frac{2}{3}°$. McIver's (2000) example can be contained between lines making angles of *ca.* 89.88° to the vertical and so certainly lies well outside the region of uniqueness of Simon & Ursell (1984), bounded by the two lines at 45° to the vertical. By considering further examples, there is the possibility of reducing the angle for which non-uniqueness occurs towards Simon & Ursell's 45° bound on uniqueness.

A different approach, and the one we adopt in this paper, to finding trapped waves in two-dimensional water waves is motivated by use of a wide-spacing argument applied to an identical pair of bodies which, in isolation, possess a zero of transmission at some particular frequency. Thus, if two submerged cylinders are placed far enough apart for neighbouring evanescent effects to be ignored, while arranging the spacing such that phases of the reflected waves coincide in the appropriate manner, one can envisage the trapping of waves between the two cylinders at that particular frequency. Just such an approach has been used by Linton & Kuznetsov (1997) for an identical pair of inclined surface-piercing plates in deep water, each of which has been shown to have zeros of transmission (Parsons & Martin 1994), and recently by Kuznetsov *et al.* (2001) for four thin vertical surface-piercing plates, based on the fact that a pair of closely spaced vertical plates has zeros of transmission (Evans & Morris 1972). The disadvantage of adopting such an approach for seeking trapped waves is two-fold. First, there are very few explicit solutions to wave-scattering problems and therefore little hope of finding explicit expressions for trapped waves in problems where the geometry is not extremely simple. Thus, trapped waves must be sought numerically with little hope of providing a rigorous proof of their existence. Secondly, unlike the inverse procedure first used by McIver (1996), the wave field at infinity is not automatically zero and so this must also be confirmed numerically. This is not an easy task, as Linton & Kuznetsov (1997) revealed, the existence of their trapped waves corresponding to a single point at which two numerically computed curves grazed each other only for certain precise geometries.

This paper uses the methods introduced in the companion paper, Porter (2002, hereafter referred to as I). In I, the two-dimensional problem of reflection of small-amplitude monochromatic waves normally incident upon an infinitely long submerged cylinder of arbitrary but uniform cross-section in a fluid of either constant depth h or of infinite depth was considered. It was shown how highly accurate estimates for the reflection coefficient could be found by formulating the problem in terms of a first-kind integral equation for a function related to the tangential velocity around the cylinder surface and approximating its solution using a Galerkin scheme. Accuracy was maintained even when the cylinders were reduced to having zero cross-section (i.e. were replaced by thin curved plates), where special test functions were employed to incorporate the known inverse square-root singularity in the velocity at the ends of the plate.

In particular, it was shown that several families of cylinder cross-section possessed the property of having frequencies at which total reflection occurred. Parsons & Martin (1994) showed that a thin flat submerged horizontal plate, if close enough to the free surface in deep water, exhibited frequencies at which there was total reflection of incident waves. In I, this result was extended in two directions, showing that zeros of transmission also exist for thin plates in fluid of finite depth and for a larger class of submerged obstacle including inclined plates, curved plates and long thin elliptical cylinders.

The method of solution is based upon the same techniques used in I for scattering by a single submerged cylinder. The problem for trapped waves above a symmetrical pair of cylinders may be reduced to a problem involving a single cylinder in a half-space with either a Neumann or a Dirichlet condition on the plane of symmetry, corresponding to symmetric and antisymmetric trapped waves, respectively. By defining an appropriate Green's function and applying Green's identity one can formulate a real integral equation of the first kind for an unknown function related to the tangential velocity around the surface of the cylinder. In addition there is a real side condition that must also be satisfied to ensure that the wave field at infinity is zero. The solution of the integral equation is approximated using the same Galerkin method shown in I to be highly accurate.

The method used to locate trapped waves is based on that of Evans & Porter (1998), who investigated embedded trapped waves in a waveguide problem, and had a similar system to solve. There, trapped waves corresponded to the solution of a real homogeneous system of equations subject to a real constraint. They showed that the trapped mode could be interpreted as the intersection of two independently computed curves, providing compelling numerical evidence for the existence of their trapped wave.

It turns out that the same technique is successful when applied to the present problem. That is, trapped waves computed for pairs of submerged cylinders correspond to the intersection of two independently computed curves. While being short of a rigorous proof of their existence (as provided, for example, by McIver (1996)), the numerical evidence presented here for the existence of trapped waves is extremely strong.

The results obtained from the present work also agree with those computed independently by C. M. Linton (1998, personal communication) for a pair of thin horizontal plates in deep water using the hypersingular integral equation approach of Parsons & Martin (1992).

2. Formulation and solution

As in I, we shall develop the formulation for the more complicated case of a pair of cylinders having non-zero cross-section, concentrating on the case of finite depth.

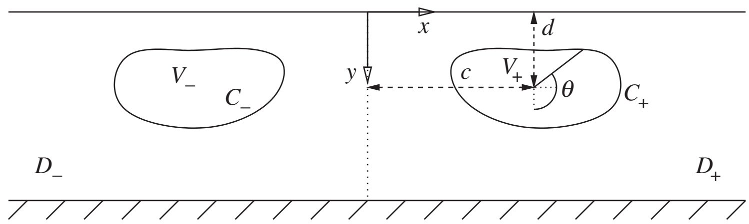

Figure 1. A symmetrical pair of submerged cylinders in fluid of constant depth, h.

Later in this section the changes required for cylinders in a fluid of infinite depth are outlined.

(*a*) *Statement of problem*

The problem is two dimensional and we work with Cartesian coordinates (x, y). These are arranged with y measured vertically downwards, $y = 0$ coinciding with the undisturbed free surface and with the fluid bottom at $y = h$. The fluid occupies the region $D_+ \cup D_-$, where $D_+ = \{x > 0,\ 0 < y < h\}\backslash V_+$ and $D_- = \{x \leqslant 0,\ 0 < y < h\}\backslash V_-$, as shown in figure 1.

A pair of cylinders of cross-section $V_\pm$ is placed symmetrically about the line $x = 0$. The boundary of the cylinder in $x > 0$ and $x < 0$ is given by the curves C_+ and C_-, respectively, described parametrically by $(x, y) = (\pm X(\theta), Y(\theta)) \in C_\pm$ for $0 \leqslant \theta \leqslant 2\pi$, where θ is measured anticlockwise from the downward vertical from the interior points (c, d) of the cylinder in $x > 0$. We shall later employ a different parametrization more suitable for symmetric pairs of thin plates.

Under the assumptions of linearized water wave theory in two-dimensions, there exists a velocity potential $\Phi(x, y, t)$ which, for time-periodic motion of angular frequency ω, can be written as

$$\Phi(x, y, t) = \mathrm{Re}\{\phi(x, y)\mathrm{e}^{-\mathrm{i}\omega t}\},$$

and ϕ satisfies

$$\nabla^2\phi \equiv \phi_{xx} + \phi_{yy} = 0, \quad \text{in } D_+ \cup D_-, \tag{2.1}$$

$$\phi_y + K\phi = 0, \quad \text{on } y = 0, \quad -\infty < x < \infty, \tag{2.2}$$

with $K = \omega^2/g$ (g is acceleration due to gravity),

$$\phi_y = 0, \quad \text{on } y = h. \tag{2.3}$$

In a fluid of infinite depth, (2.3) is replaced by

$$\phi, \nabla\phi \to 0, \quad \text{as } y \to \infty.$$

Also,

$$\phi_\mathrm{n} = 0, \quad \text{on } (x, y) \in C_+ \cup C_-, \tag{2.4}$$

the subscript 'n' denoting the normal derivative from $D_\pm$ into $C_\pm$. For trapped waves, there are no incoming or outgoing waves at infinity, so that

$$\phi \to 0, \quad \text{as } |x| \to \infty. \tag{2.5}$$

On account of the symmetry in the geometry about $x = 0$, we may consider symmetric and antisymmetric motions independently, defined by the potentials $\phi^{\mathrm{s,a}}(x, y)$ satisfying (2.1)–(2.5) and

$$\phi^{\mathrm{s,a}}(x, y) = \pm\phi^{\mathrm{s,a}}(-x, y), \tag{2.6}$$

where the superscript 's' refers to the upper sign and superscript 'a' refers to the lower sign. Thus, we may restrict attention to the semi-infinite domain $D \equiv D_+$ involving just one cylinder by imposing the boundary conditions

$$\frac{\partial \phi^{\mathrm{s}}}{\partial x} = 0, \quad \phi^{\mathrm{a}} = 0, \quad \text{on } x = 0, \tag{2.7}$$

and recovering the wave field in D_- from (2.6). The no-flow condition (2.4) is now imposed only on the cylinder boundary $C_+ \equiv C$.

Finally, since ϕ satisfies Laplace's equation with homogeneous boundary conditions, we may take ϕ, and therefore $\phi^{\mathrm{s,a}}$, to be real without any loss of generality.

(*b*) *Wide spacing*

Before developing an exact formulation of the problem defined above we first use the so-called wide-spacing argument, described briefly in § 1, to motivate the search for trapped waves and to provide approximations to the wavenumber and spacing at which they may be expected to occur. First, consider the problem in I: the scattering of incident waves by a single submerged obstacle centred on the line $x = 0$. The velocity potential for this problem, ϕ_{scat}, say, as $x \to \infty$ due to a wave of wavenumber k incident from $x = \infty$ is given by

$$\phi_{\mathrm{scat}}(x, y) \sim (\mathrm{e}^{-\mathrm{i}kx} + R\mathrm{e}^{\mathrm{i}kx})d(y), \tag{2.8}$$

where R is the reflection coefficient, $d(y)$ is a function dependent upon the depth of the fluid and k is related to frequency through the dispersion relation

$$K = \omega^2/g = k \tanh kh$$

(note $k = K$ in infinite depth). For certain submerged obstacles, it was shown that there exists a wavenumber $k = \tilde{k}$, say, for which $|R| = 1$ so that R is expressible in terms of its phase, 2σ, by writing

$$R = \mathrm{e}^{2\mathrm{i}\sigma}.$$

Now place a second cylinder symmetrically about a plane $x = \tilde{c}$ and centred on $x = 2\tilde{c}$, where $\tilde{c} \gg 1$ so that evanescent modes from wave interactions at each obstacle may be neglected. By arranging the spacing $2\tilde{c}$ so that the phase of the reflected wave matches correctly at each obstacle, a wave of wavenumber $k = \tilde{k}$ travelling between the obstacles will make permanent reflections and therefore be trapped. As previously mentioned, we may consider trapped waves that are either symmetric (ϕ^{s}) or antisymmetric (ϕ^{a}) about the plane of symmetry between them. Thus, the approximate condition for symmetric trapped waves is given by

$$\frac{\partial}{\partial x}\phi_{\mathrm{scat}}(\tilde{c}, y) = 0,$$

and for antisymmetric trapped waves

$$\phi_{\text{scat}}(\tilde{c}, y) = 0,$$

where ϕ_{scat} assumes its asymptotic form given by (2.8). These two conditions imply the relations

$$\sigma = n\pi + \tilde{k}\tilde{c}, \qquad n \in \mathbb{Z} \quad \text{(symmetric modes)},$$
$$\sigma = (n + \tfrac{1}{2})\pi + \tilde{k}\tilde{c}, \quad n \in \mathbb{Z} \quad \text{(antisymmetric modes)},$$

which provide approximations to the wavenumber and spacings between pairs of cylinders for trapped waves in terms of the wavenumber and phase of the reflection coefficient at which total reflection occurs.

The argument described above is heuristic and gives approximations to trapped-wave parameters. Hereafter we formulate the problem exactly.

(c) *Formulation of integral equations: finite depth*

The notation that follows is defined in § 2 of I. We seek the real potential $\phi \equiv \phi^{\mathrm{s,a}}$ satisfying (2.1)–(2.5) in $x > 0$ with (2.7). To do this, we define the Green's functions

$$G^{\mathrm{s,a}}(x, y \mid x_0, y_0) = \mathrm{Re}\{G(x, y \mid x_0, y_0) \pm G(-x, y \mid x_0, y_0)\},$$

where G is defined in (2.13) in I, for the symmetric and antisymmetric problems, respectively, and satisfying

$$\frac{\partial}{\partial x} G^{\mathrm{s}}(0, y \mid x_0, y_0) = 0, \qquad G^{\mathrm{a}}(0, y \mid x_0, y_0) = 0.$$

Thus, for $x, x_0 \geqslant 0$,

$$G^{\mathrm{s,a}}(x, y \mid x_0, y_0) = \frac{\psi_0(y)\psi_0(y_0)}{2kh}(\sin k|x - x_0| \pm \sin k(x + x_0)) + \sum_{m=1}^{\infty} \frac{\psi_m(y)\psi_m(y_0)}{2k_m h}(\mathrm{e}^{-k_m|x - x_0|} \pm \mathrm{e}^{-k_m(x + x_0)}), \tag{2.9}$$

with superscripts 's' and 'a' corresponding to upper and lower signs, respectively. Here we have used k_m to denote the real positive roots of $K = -k_m \tan k_m h$, $m \geqslant 1$, with $k_0 = -\mathrm{i}k$ and

$$\psi_m(y) = N_m^{-1/2} \cos k_m(h - y), \qquad N_m = \tfrac{1}{2}(1 + \sin(2k_m h)/(2k_m h)).$$

The Green's functions defined in (2.9) have a standing-wave behaviour at infinity (given by the first term in (2.9)) and the use of $G^{\mathrm{s,a}}$ in Green's identity will not automatically ensure that $\phi^{\mathrm{s,a}} \to 0$ as $x \to \infty$. The vanishing of the far field at infinity will require a further condition to be placed on $\phi^{\mathrm{s,a}}$ which cancels the standing-wave contributions from $G^{\mathrm{s,a}}$ at infinity.

Applying Green's identity (eqn (2.15) in I) to $\phi \equiv \phi^{\mathrm{s,a}}$ and $G \equiv G^{\mathrm{s,a}}$ in turn on the domain $D' : \{0 < x < X,\ 0 < y < h\} \backslash V_+$, then taking the limit $X \to \infty$ by means of (2.5), we find that

$$\phi^{\mathrm{s,a}}(x_0, y_0) = -\int_C \phi^{\mathrm{s,a}}(x, y) \frac{\partial}{\partial n} G^{\mathrm{s,a}}(x, y \mid x_0, y_0)\, \mathrm{d}s, \quad (x_0, y_0) \in D. \tag{2.10}$$

Taking the limit $x_0 \to \infty$, using (2.5) and (2.9), shows that the potential on the cylinder must also satisfy the condition

$$0 = \int_C \phi^{\mathrm{s,a}}(x,y)\frac{\partial}{\partial n}\left(\psi_0(y)\begin{Bmatrix}\cos kx\\ \sin kx\end{Bmatrix}\right)\mathrm{d}s, \tag{2.11}$$

where the upper (respectively, lower) entry in the braces refers to the symmetric (respectively, antisymmetric) problem.

Hereafter, we follow the method used in I. It is a straightforward matter to confirm that

$$\frac{\partial^2}{\partial n_0 \partial n}G^{\mathrm{s,a}}(x,y \mid x_0,y_0) = -\frac{\partial^2}{\partial s_0 \partial s}H^{\mathrm{s,a}}(x,y \mid x_0,y_0), \tag{2.12}$$

for $(x,y) \neq (x_0,y_0)$, where

$$\begin{aligned} H^{\mathrm{s,a}}(x,y \mid x_0,y_0) = {} & \frac{\chi_0(y)\chi_0(y_0)}{2kh}(\sin k|x-x_0| \mp \sin k(x+x_0)) \\ & + \sum_{m=1}^{\infty}\frac{\chi_m(y)\chi_m(y_0)}{2k_m h}(\mathrm{e}^{-k_m|x-x_0|} \mp \mathrm{e}^{-k_m(x+x_0)}), \end{aligned} \tag{2.13}$$

using the relations (2.16) in I, where $\chi_m(y)$ are defined by

$$\chi_m(y) = N_m^{-1/2}\sin k_m(h-y), \quad m = 0,1,\ldots$$

(see eqn (2.15) in I). Also, the stream function $\psi^{\mathrm{s,a}}(x,y)$ is related via the Cauchy–Riemann equations to $\phi^{\mathrm{s,a}}(x,y)$ using (2.16) in I by

$$\frac{\partial}{\partial n}\phi^{\mathrm{s,a}}(x,y) = -\frac{\partial}{\partial s}\psi^{\mathrm{s,a}}(x,y). \tag{2.14}$$

First, taking the normal derivative $\partial/\partial n_0$ at the point (x_0,y_0) in (2.10), substituting from (2.12) and (2.13) and integrating with respect to s_0 gives

$$\psi^{\mathrm{s,a}}(x_0,y_0) = -\int_C \phi^{\mathrm{s,a}}(x,y)\frac{\partial}{\partial s}H^{\mathrm{s,a}}(x,y \mid x_0,y_0)\,\mathrm{d}s, \quad (x_0,y_0) \in D.$$

Then integration by parts transfers the tangential derivative from $H^{\mathrm{s,a}}$ to $\phi^{\mathrm{s,a}}$ to give

$$\int_C H^{\mathrm{s,a}}(x,y \mid x_0,y_0)\frac{\partial}{\partial s}\phi^{\mathrm{s,a}}(x,y)\,\mathrm{d}s = \psi^{\mathrm{s,a}}(x_0,y_0), \quad (x_0,y_0) \in D, \tag{2.15}$$

since the function $\phi^{\mathrm{s,a}}$ is continuous on C. Moving the point (x_0,y_0) onto C gives

$$\int_C H^{\mathrm{s,a}}(x,y \mid x_0,y_0)\frac{\partial}{\partial s}\phi^{\mathrm{s,a}}(x,y)\,\mathrm{d}s = \psi_C^{\mathrm{s,a}}, \quad (x_0,y_0) \in C, \tag{2.16}$$

where $\psi_C^{\mathrm{s,a}}$ is the *constant* value of the stream function on the cylinder boundary C. As in I (cf. eqn (3.11)), we introduce the parametrization of the cylinder surface at this point by writing

$$q^{\mathrm{s,a}}(\theta) = \left[X'(\theta)\frac{\partial}{\partial x} + Y'(\theta)\frac{\partial}{\partial y}\right]\phi^{\mathrm{s,a}}(X(\theta),Y(\theta)), \quad 0 \leqslant \theta < 2\pi,$$

which is related to the tangential fluid velocity on the surface of the cylinder, and employ the shorthand notation

$$H^{\mathrm{s,a}}(\theta \mid \theta_0) \equiv H^{\mathrm{s,a}}(X(\theta), Y(\theta) \mid X(\theta_0), Y(\theta_0)), \quad 0 \leqslant \theta,\ \theta_0 < 2\pi.$$

Then (2.16) can be written as the equation

$$(\mathcal{K}^{\mathrm{s,a}} q^{\mathrm{s,a}})(\theta_0) = \psi_C^{\mathrm{s,a}} \tag{2.17}$$

in $L_2(0, 2\pi)$, where

$$(\mathcal{K}^{\mathrm{s,a}} q)(\theta_0) = \int_0^{2\pi} q(\theta) H^{\mathrm{s,a}}(\theta \mid \theta_0)\, \mathrm{d}\theta. \tag{2.18}$$

We also require that $q^{\mathrm{s,a}}(\theta)$ be continuous ($q^{\mathrm{s,a}}(2\pi) = q^{\mathrm{s,a}}(0)$) and impose continuity of $\phi^{\mathrm{s,a}}$ on C, which can be written as

$$(q^{\mathrm{s,a}}, 1) = 0, \tag{2.19}$$

where the inner product notation

$$(u, v) = \int_0^{2\pi} u(\theta) v(\theta)\, \mathrm{d}\theta \tag{2.20}$$

for real elements $u, v \in L_2(0, 2\pi)$ has been used.

Finally, we return to the supplementary condition that the far field vanishes at large distances, by transferring from normal derivatives to tangential derivatives in (2.11) to give

$$0 = \int_C \phi^{\mathrm{s,a}}(x, y) \frac{\partial}{\partial s}\left(\mathrm{i}\chi_0(y) \begin{Bmatrix} \sin kx \\ \cos kx \end{Bmatrix}\right) \mathrm{d}s.$$

Integrating by parts and employing the parametrization in terms of θ gives

$$0 = (q^{\mathrm{s,a}}, f^{\mathrm{s,a}}) \equiv \int_0^{2\pi} q^{\mathrm{s,a}}(\theta) f^{\mathrm{s,a}}(\theta)\, \mathrm{d}\theta, \tag{2.21}$$

where we have defined the (real) functions

$$f^{\mathrm{s}}(\theta) = \mathrm{i}\chi_0(Y(\theta)) \sin kX(\theta), \qquad f^{\mathrm{a}}(\theta) = \mathrm{i}\chi_0(Y(\theta)) \cos kX(\theta). \tag{2.22}$$

Trapped waves therefore correspond to non-trivial solutions of (2.17) subject to (2.19) and (2.21).

(d) *Infinite depth*

We refer the reader to § 5 of I in which modifications were made in the scattering problem in finite depth to consider the case of infinite depth. The Green's functions appropriate to the symmetric and antisymmetric problems are defined by

$$G_\infty^{\mathrm{s,a}}(x, y \mid x_0, y_0) = \mathrm{Re}\{G_\infty(x, y \mid x_0, y_0) \pm G_\infty(-x, y \mid x_0, y_0)\},$$

where G_∞ is given in I, and leads to

$$\begin{aligned} G_\infty^{\mathrm{s,a}}(x, y \mid x_0, y_0) = -\frac{1}{2\pi}\left\{\log\left(\frac{r_0}{r_1}\right) \pm \log\left(\frac{r_2}{r_3}\right)\right\} \\ - \frac{1}{\pi} ⨍_0^\infty \frac{\mathrm{e}^{-\nu(y+y_0)}}{K - \nu}\{\cos\nu(x - x_0) \pm \cos\nu(x + x_0)\}\, \mathrm{d}\nu. \end{aligned} \tag{2.23}$$

The integral in the above expression is Cauchy principal-valued and $r_0^2 = (x-x_0)^2 + (y-y_0)^2$, $r_1^2 = (x-x_0)^2+(y+y_0)^2$ as in eqn (5.1) in I, while $r_2^2 = (x+x_0)^2+(y-y_0)^2$, $r_3^2 = (x+x_0)^2 + (y+y_0)^2$. Also, the far-field behaviour of the Green's functions is given by the standing-wave behaviour

$$G_\infty^{\mathrm{s,a}}(x, y \mid x_0, y_0) \sim -\mathrm{e}^{-K(y+y_0)}\{\sin K|x-x_0| \pm \sin K(x+x_0)\}, \quad |x-x_0| \to \infty,$$

which can be found by indenting the integral around the pole at $\nu = K$ in (2.23). In accordance with the method used in finite depth, $H_\infty^{\mathrm{s,a}}$ is defined by

$$\frac{\partial^2}{\partial n_0 \partial n} G_\infty^{\mathrm{s,a}}(x, y \mid x_0, y_0) = -\frac{\partial^2}{\partial s_0 \partial s} H_\infty^{\mathrm{s,a}}(x, y \mid x_0, y_0),$$

giving

$$H_\infty^{\mathrm{s,a}}(x, y \mid x_0, y_0) = -\frac{1}{2\pi}\{\log(r_0 r_1) \mp \log(r_2 r_3)\} + \frac{1}{\pi} \int_0^\infty \frac{\mathrm{e}^{-\nu(y+y_0)}}{K-\nu}\{\cos\nu(x-x_0) \mp \cos\nu(x+x_0)\}\,\mathrm{d}\nu,$$

which can be confirmed using eqns (2.14) and (2.16) from I with $m = 0$.

The development of the formulation described previously for the case of finite depth is unchanged in the case of infinite depth, apart from a slightly different far-field behaviour. It turns out that trapped waves in infinite depth require (2.17) to be satisfied with $H_\infty^{\mathrm{s,a}}$ replacing $H^{\mathrm{s,a}}$ in the definition of (2.18), subject to (2.19) and such that (2.21) is also satisfied where, in this case, the functions $f^{\mathrm{s,a}}$ defined by (2.22) are replaced by

$$f^{\mathrm{s}}(\theta) = \mathrm{e}^{-KY(\theta)} \sin kX(\theta), \qquad f^{\mathrm{a}}(\theta) = \mathrm{e}^{-KY(\theta)} \cos kX(\theta).$$

(*e*) *Thin plates*

The changes required to formulate the problem for thin plates are similar to those described in I. Briefly, the curve C is replaced by a line L parametrized by $(x, y) = (X(t), Y(t))$, $-1 \leqslant t \leqslant 1$. The integral operator in (2.18) is replaced by

$$(\mathcal{K}^{\mathrm{s,a}})q(t_0) = \int_{-1}^{1} q(t) H^{\mathrm{s,a}}(t \mid t_0)\,\mathrm{d}t,$$

on $L_2(-1, 1)$, where $H^{\mathrm{s,a}}(t \mid t_0) = H^{\mathrm{s,a}}(X(t), Y(t) \mid X(t_0), Y(t_0))$ and

$$q^{\mathrm{s,a}}(t) = \sigma(t)[\phi_s^{\mathrm{s,a}}(X(t), Y(t))]_L,$$

the square brackets indicating the jump in ϕ_s across the plate L, and $\sigma^2(t) = (X'(t))^2 + (Y'(t))^2$. The definition of the inner product is replaced by

$$(u, v) = \int_{-1}^{1} u(t)v(t)\,\mathrm{d}t \tag{2.24}$$

for real functions $u, v \in L_2(-1, 1)$. The function $q^{\mathrm{s,a}}(t)$ has singular inverse square-root behaviour at $t = \pm 1$ (i.e. at the ends of the plate). We simply replace $H^{\mathrm{s,a}}$ by $H_\infty^{\mathrm{s,a}}$ in the above for infinite depth.

3. Approximation and numerical method

In this section we initially suppress the superscript 's,a' from the various quantities. As in I, we approximate the unknown function q by writing

$$q \approx \tilde{q} = \sum_{n=1}^{2N} a_n u_n \tag{3.1}$$

in terms of the set of functions $\{u_n\}$, $n = 0, 1, \dots$, which are real and satisfy

$$(u_n, 1) = 0, \quad n = 1, \dots, 2N, \tag{3.2}$$

ensuring that the approximation to q satisfies (2.19). Also, u_0 is chosen such that $(u_0, 1) \neq 0$. The set of real coefficients $\{a_n\}$, $n = 1, \dots, 2N$, and the value of ψ_C are determined by solving

$$(\mathcal{K}\tilde{q} - \psi_C, u_m) = 0, \quad m = 0, 1, 2, \dots, 2N,$$

a process which characterizes Galerkin's method. Substitution of (3.1) therefore results in the system of real equations

$$\sum_{n=1}^{2N} a_n K_{mn} = 0, \quad m = 1, 2, \dots, 2N, \tag{3.3}$$

on account of (3.2) with the $m = 0$ equation giving

$$\sum_{n=1}^{2N} a_n K_{0n} = (u_0, 1)\psi_C, \tag{3.4}$$

which determines ψ_C in terms of the coefficients $\{a_n\}$ defined by (3.3). Here, we have written

$$K_{mn} = (\mathcal{K}u_n, u_m). \tag{3.5}$$

Numerical approximations to trapped-wave solutions are provided by the non-trivial solutions to (3.3), which must also satisfy the supplementary condition (2.21). After use of the approximation (3.1), this condition becomes

$$S \equiv \sum_{n=1}^{2N} a_n (u_n, f) = 0. \tag{3.6}$$

The set of functions, $\{u_n\}$, introduced in I are unchanged. Thus, for submerged cylinders having a smooth boundary, the Fourier series is appropriate;

$$u_{2n}(\theta) = \cos n\theta, \quad u_{2n-1}(\theta) = \sin n\theta, \quad \text{for } n = 1, 2, \dots, \tag{3.7}$$

and $u_0 = \frac{1}{2}$, each function being continuous, real, periodic and satisfying (3.2) for $n \geqslant 1$ as required. If the submerged obstacle is a thin plate, weighted orthogonal Chebychev polynomials are used, to account for the singularity at the ends of the plate. Thus,

$$u_n(t) = (1 - t^2)^{-1/2} T_n(t), \quad -1 < t < 1, \quad n = 0, 1, 2, \dots, \tag{3.8}$$

such that $(u_0, 1) = \pi$ while satisfying (3.2) for $n \geqslant 1$.

We give brief details about the procedure needed to compute K_{mn} in (3.5), firstly in the case of finite depth and described for a cylinder with non-zero cross-section. From (3.5) and the definition of the integral operator in (2.18) with (2.13) we have

$$K_{mn}^{\mathrm{s,a}} = K_{mn}^{(\mathrm{w})} + K_{mn}^{(\mathrm{e})} \pm \frac{1}{2kh}(F_n^{\mathrm{s}}F_m^{\mathrm{a}} + F_n^{\mathrm{a}}F_m^{\mathrm{s}}) \mp \sum_{r=1}^{\infty} \frac{G_{nr}G_{mr}}{2k_n h},$$

where the superscript 's' (respectively, 'a') refers to the upper (respectively, lower) sign. Here, $F_n^{\mathrm{s,a}} = (u_n, f^{\mathrm{s,a}})$,

$$G_{nr} = \int_0^{2\pi} u_n(\theta)\chi_r(Y(\theta))\mathrm{e}(-k_r X(\theta))\,\mathrm{d}\theta,$$

which, since $k_r \sim r\pi$ as $r \to \infty$, tend to zero rapidly as r increases, while

$$K_{mn}^{(\mathrm{w})} = \frac{1}{2kh}\int_0^{2\pi} u_m(\theta_0)\chi_0(Y(\theta_0))\int_0^{2\pi} u_n(\theta)\chi_0(Y(\theta))\sin k|X(\theta) - X(\theta_0)|\,\mathrm{d}\theta\,\mathrm{d}\theta_0 \tag{3.9}$$

and

$$K_{mn}^{(\mathrm{e})} = \int_0^{2\pi} u_m(\theta_0)\int_0^{2\pi} u_n(\theta)\sum_{r=1}^{\infty}\frac{\chi_r(Y(\theta))\chi_r(Y(\theta_0))}{2k_r h}\mathrm{e}^{-k_r|X(\theta)-X(\theta_0)|}\,\mathrm{d}\theta\,\mathrm{d}\theta_0. \tag{3.10}$$

Finally, the factors $F_n^{\mathrm{s,a}}$ are precisely those needed for computing S. Suppressing superscripts 's' and 'a', (3.6) is

$$S \equiv \sum_{n=1}^{2N} a_n F_n = 0. \tag{3.11}$$

In (3.10), $K_{mn}^{(\mathrm{e})}$ is precisely the same as in I, eqn (4.10) and its computation is described in detail in I. There are no difficulties in computing other terms needed for $K_{mn}^{\mathrm{s,a}}$.

In infinite depth, there are no numerical difficulties in addition to those already discussed in I. The kernel, $H_\infty^{\mathrm{s,a}}$ can be treated numerically by dividing into four parts, such that

$$K_{mn}^{\mathrm{s,a}} = K_{mn}^{(\mathrm{s})} + K_{mn}^{(\mathrm{r})} \pm (K_{mn}^{(\mathrm{s}')} + K_{mn}^{(\mathrm{r}')})$$

where $K_{mn}^{(\mathrm{s})}$ and $K_{mn}^{(\mathrm{r})}$ are precisely those defined in I, eqn (5.7), and

$$K_{mn}^{(\mathrm{s}')} = -\frac{1}{2\pi}\int_0^{2\pi} u_m(\theta_0)\int_0^{2\pi} u_n(\theta)\log(r_2 r_3)\,\mathrm{d}\theta\,\mathrm{d}\theta_0,$$

$$K_{mn}^{(\mathrm{r}')} = -\frac{1}{\pi}\int_0^{2\pi} u_m(\theta_0)\int_0^{2\pi} u_n(\theta) \times \left[⨍_0^{\infty} \frac{\mathrm{e}^{-\nu(Y(\theta)+Y(\theta_0))}}{K-\nu}\cos\nu(X(\theta)+X(\theta_0))\,\mathrm{d}\nu\right]\mathrm{d}\theta\,\mathrm{d}\theta_0.$$

The computation of $K_{mn}^{(\mathrm{r})}$ and $K_{mn}^{(\mathrm{r}')}$ is aided by the expansion of the principal-value integral described in Yu & Ursell (1961) and written explicitly in eqn (5.4) in I for

Table 1. *A selection of numerical results found by C. M. Linton (1998, personal communication) for trapped waves supported by a pair of submerged horizontal plates*

d/a	Ka	c/a
0.05	0.393	1.621
0.1	0.620	1.590
0.1	0.618	6.707
0.15	0.717	1.717
0.2	0.379	4.115
0.2	0.701	2.008
0.2	0.671	6.816

the former of these two elements. There is no difficulty computing either of these elements, nor $K_{mn}^{(s')}$; the only element over which care needs to be taken is $K_{mn}^{(s)}$, and this process is described in detail in § 5 of I.

All integrals are computed numerically using ten-point Gauss–Legendre quadrature with 100 evaluations of the integrand. This is usually sufficient to claim eight-figure accuracy in the various elements being computed.

4. Results

At the end of § 1 it was mentioned briefly that trapped-wave results have already been obtained for thin submerged horizontal plates by C. M. Linton (1998, personal communication) using the hypersingular integral equation approach of Parsons & Martin (1994). However, Linton's method did not establish conclusive numerical evidence for the existence of trapped waves, since they correspond to a single point at which two numerically generated curves met one another tangentially only for precise geometrical configurations. Numerical inaccuracies meant that the curves never actually touched, but got closer as the numerical scheme increased in accuracy. A selection of Linton's results are given in table 1. These results have been confirmed using the present method.

The submerged obstacles used in the present paper were given in I. We use a pair of elliptical cylinders and a pair of flat inclined plates, the obstacle in $x > 0$ described parametrically by

(i) elliptical cylinder: $X(\theta) = c + a\sin\theta$, $Y(\theta) = d + b\cos\theta$, $0 \leqslant \theta < 2\pi$,

(ii) flat inclined plate: $X(t) = c + at\cos\delta$, $Y(t) = d + a(1+t)\sin\delta$, $-1 \leqslant t \leqslant 1$.

Clearly, we must have $c/a > 1$ for there to be a gap between the submerged pair of obstacles.

We now describe the method for determining trapped waves, which we base on the method used by Evans & Porter (1998) for a similar problem where trapped modes embedded in the continuous spectrum were determined for a circular cylinder in a waveguide.

We are required to seek non-trivial solutions of (3.3) which simultaneously satisfy (3.6). The procedure we adopt is as follows. For a particular chosen pair of submerged obstacles of fixed dimensions, the non-trivial solutions of (3.3) are determined by

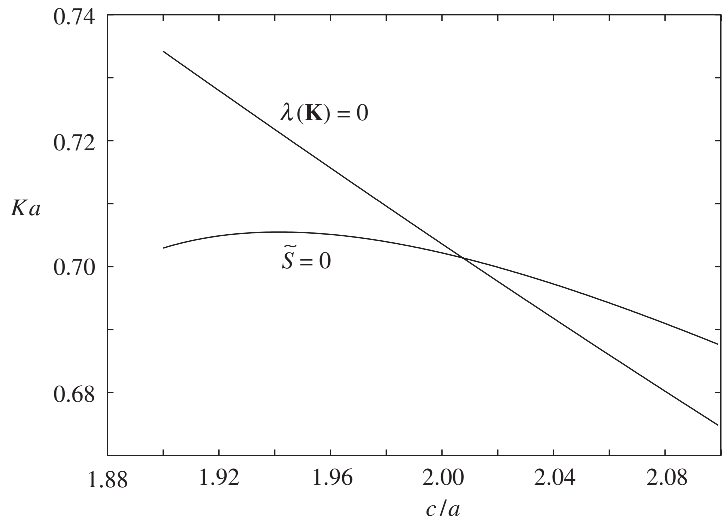

Figure 2. Curves of $\lambda(\boldsymbol{K}) = 0$ and $\tilde{S} = 0$ in $(Ka, c/a)$ parameter space for a pair of thin horizontal flat plates in infinite depth with $a/d = 5$.

locating zeros of the real eigenvalues of the matrix $\boldsymbol{K}$ of elements K_{mn} in (3.5). Provided a suitable set of parameters is chosen, this procedure results in a curve of the variation of non-dimensional frequency Ka as a function of the spacing c/a on which (3.3) has non-trivial solutions. This curve is labelled as $\lambda(\boldsymbol{K}) = 0$ in the example shown in figure 2. A second curve generated independently of this first curve is labelled $\tilde{S} = 0$ in figure 2 and represents the vanishing of the real quantity $\tilde{S}$, defined to be

$$\tilde{S} = \sum_{n=1}^{2N} \tilde{a}_n (u_n, f_n).$$

Here, $\tilde{a}_n$, $n = 1, \ldots, 2N$, are elements of the eigenvector corresponding to the smallest (real) eigenvalue of the matrix $\boldsymbol{K}$. At the point where the two curves cross, the value of the smallest eigenvalue is zero and so $a_n = \tilde{a}_n$. Therefore the point of intersection of the two curves corresponds to a trapped wave and its location in $(Ka, c/a)$ space gives the precise frequency and spacing at which the trapped wave occurs. The procedure described above is numerically robust, since the curves are computed independently of one another and lack of accuracy in the approximation and/or numerical rounding errors do not result in the crossing point being lost.

In figure 2, curves of $\lambda(\boldsymbol{K}) = 0$ and $\tilde{S} = 0$ are shown for a pair of submerged plates of length $a/d = 5$ in a fluid of infinite depth. The precise crossing point is at $(Ka, c/a) = (0.701\,378, 2.007\,460)$ in close agreement with values computed by Linton in table 1.

A demonstration of the accuracy of the results is given in table 2, where two examples are chosen to test the method: a pair of thin horizontal plates of length $a/d = 10$ in infinite depth and a pair of long thin elliptical cylinders, again of length $a/d = 10$, and with width $b/a = 0.02$ and submergence depth $d/h = 10$. These two examples use sets of functions u_n defined by (3.8) and (3.7), respectively. Convergence for the thin horizontal plate is excellent with six-figure accuracy in values of Ka and spacing, c/a, being reached with only ten terms in the expansion. The example involving the thin elliptical cylinders requires a truncation size of 16 to reach a similar accuracy due to the fact that Fourier series are being used to model large localized peaks in tangential velocities at the two high-curvature ends of the cylinder cross-section. Notice that the results for the horizontal plate with $a/d = 10$ are in agreement with Linton's results in table 1. A value of $2N = 16$ was used for producing the results in the remainder of the paper.

The task of actually finding examples of submerged obstacles that support trapped waves is not trivial. There are several parameters which can be varied and trapped waves only exist for specific configurations at specific frequencies. To assist, we use the results of the wide-spacing argument described in § 2. These give us approximate values of Ka and c/a for a given pair of cylinders using information from the scattering by a single cylinder which have zeros of transmission.

To demonstrate how good the wide-spacing approximations are, notice the striking similarity between the curves shown in parts (a) and (b) of figure 3. Figure 3a shows approximate values $\tilde{K}a$ and $\tilde{c}/a$ predicted from wide spacing, while figure 3b shows the 'exact' values of Ka and c/a computed for a range of submerged obstacle pairings. Each of the curves labelled (i), (ii) and (iii) represents a family of obstacle pairing, all in infinite depth. Thus (i) is for a horizontal plate, (ii) and (iii) for an elliptical cross-section of aspect ratio $b/a = 0.08$ and 0.16, respectively. Each point on the curves represents the values of Ka and c/a at which trapped waves exist for a particular value of obstacle length, a/d, and the curve therefore shows the locus in $(Ka, c/a)$ parameter space of trapped-wave results as a/d varies.

Each curve is divided into solid and dotted sections. The point at which they meet indicates that the minimum value of a/d has been reached on that particular curve. In figure 3a, b, integer values of a/d are also marked against the open squares on the curves with plus signs denoting sub-intervals of 0.1 in a/d.

For each submerged obstacle pairing, there are two sets of curves shown in figure 3a, b. Those for smaller values of c/a correspond to *symmetric* trapped waves, while the set of curves to the right of the figures correspond to *antisymmetric* trapped waves. By increasing the separation, further trapped waves can be found alternating between symmetric and antisymmetric modes as c/a increases. Also, the wide-spacing results show better agreement as the separation, c/a, is increased, as might be expected. The largest discrepancy between the wide-spacing approximation and computed results is for smaller values of c/a. For example, while wide spacing predicts that trapped waves exist for $a/d \gtrsim 4.48$ in the case of a horizontal plate (curve (i)), corresponding to plates that have zeros of transmission, the 'exact' results show that there are, in fact, trapped waves for $a/d \gtrsim 4.32$. In contrast, for the first antisymmetric mode, trapped waves fail to exist for $a/d \lesssim 4.53$. Thus, although there is a clear link between the trapped waves being investigated here and zeros of transmission for individual submerged obstacles, it has been shown that the property of total reflection is neither necessary nor sufficient for the existence of pairs of submerged trapping obstacles.

A similar set of results is presented in figure 4, this time showing the effect of the depth of the fluid on the existence of trapped waves and the values of Ka and c/a for which they occur. As in the previous example, the curves labelled (i), (ii) and (iii) are for a flat horizontal plate, and elliptical cylinders with aspect ratios $b/a = 0.08$ and 0.16, respectively, and with the lengths fixed at $a/d = 5$. Wide-spacing results are

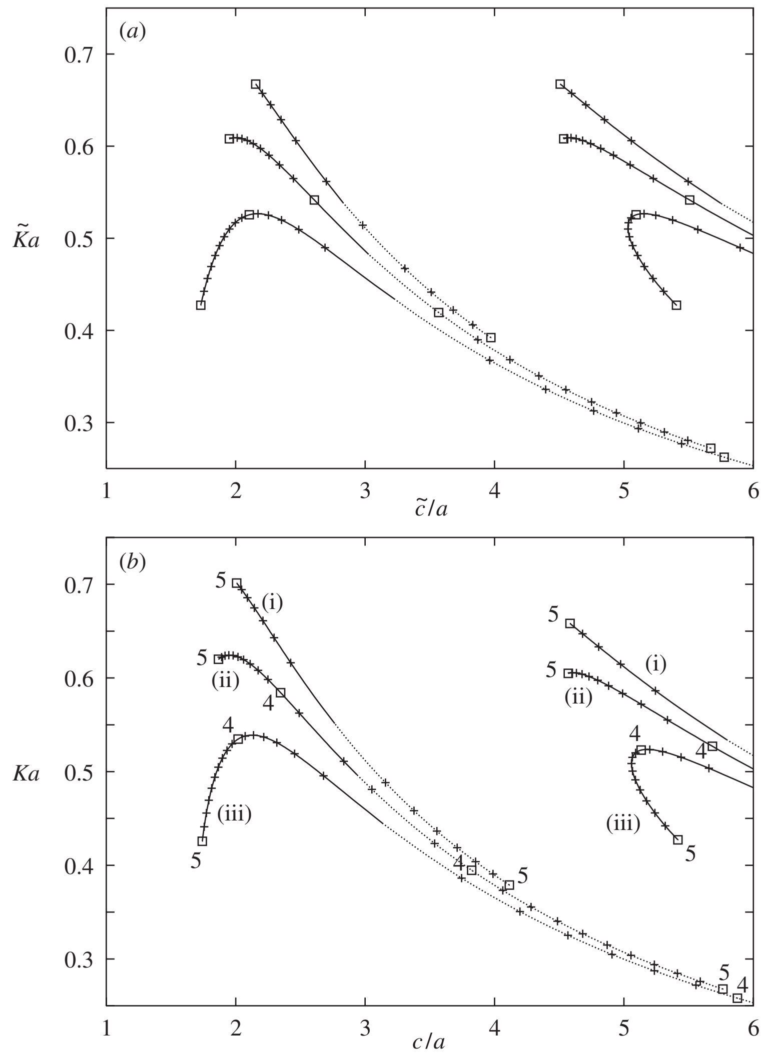

Figure 3. The locus of trapped waves in $(Ka, c/a)$ parameter space as the length a/d of the pair of submerged ellipses is varied: (a) as predicted by wide-spacing arguments; and (b) computed values ((i) $b/a = 0$ (flat plate), (ii) $b/a = 0.08$, (iii) $b/a = 0.16$). Integer values of a/d are labelled against open squares, and the plus signs denote intervals of 0.1.

used as initial guesses, and are readily available from the computations performed in I. The end points of the curves in figure 4 marked by open squares are results for infinite depth and each plus sign along the curve from these points represents an increase in depth d/h of 0.025. As before, the junction of the solid and dotted sections of the curve indicates where d/h has reached its maximum for that particular obstacle pairing. For example, symmetric trapped waves exist for a horizontal flat plate provided the depth is $d/h \lesssim 0.121$. Also, the curves for smaller (respectively, larger) values of c/a correspond to symmetric (respectively, antisymmetric) trapped waves, and further symmetric and antisymmetric trapped waves also exist as the spacing c/a increases (not shown in figure 4).

Table 2. *Convergence of numerical scheme for two cases: (i) a pair of horizontal plates in infinite depth, and (ii) a pair of thin ellipses in finite depth*

	horizontal plate in infinite depth: $a/d = 10$		thin ellipse in finite depth: $a/d = 10$, $b/a = 0.02$, $d/h = 0.1$	
$2N$	Ka	c/a	Ka	c/a
2	0.643 847	1.727 608	—	—
4	0.619 802	1.593 672	0.541 138	1.506 397
6	0.619 874	1.589 583	0.573 134	1.241 194
8	0.619 874	1.589 577	0.526 908	1.291 444
10	0.619 873	1.589 578	0.526 695	1.284 989
12			0.526 295	1.285 454
14			0.526 298	1.285 420
16			0.526 298	1.285 420

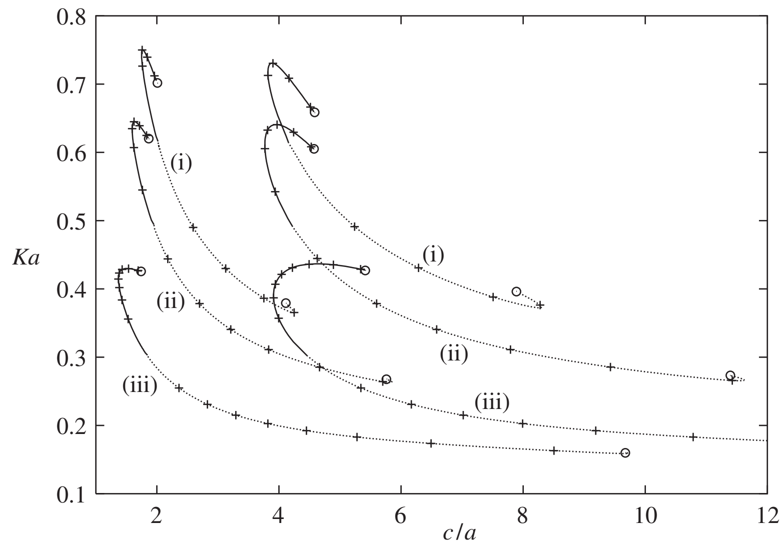

Figure 4. The locus of trapped waves in $(Ka, c/a)$ parameter space as the depth d/h of the fluid is varied for a pair of submerged ellipses length $a/d = 5$: (i) $b/a = 0$ (flat plate), (ii) $b/a = 0.08$, (iii) $b/a = 0.16$. Infinite-depth results are marked with open circles and intervals of 0.025 in d/h are marked by plus signs.

Finally, in figure 5 curves show the variation of Ka and c/a at which trapped waves occur with the angle of inclination, δ, for a flat plate of length (i) $a/d = 5$, (ii) $a/d = 7.5$ and (iii) $a/d = 10$. As in the previous two examples, use is made of the computations performed in I to provide approximations to trapped waves using the wide-spacing expressions of § 2. The endpoints of each curve (open circles) are for $\delta = 0°$ and each plus sign marked along the curve represents an increase of 1° up to the point at which solid and dotted sections of the curve meet, at which point the trapped wave ceases to exist. Figure 5 shows that longer plates can be inclined at a greater angle before the trapped wave ceases to exist, although the values of Ka and c/a at which this happens are similar for all three plate lengths considered.

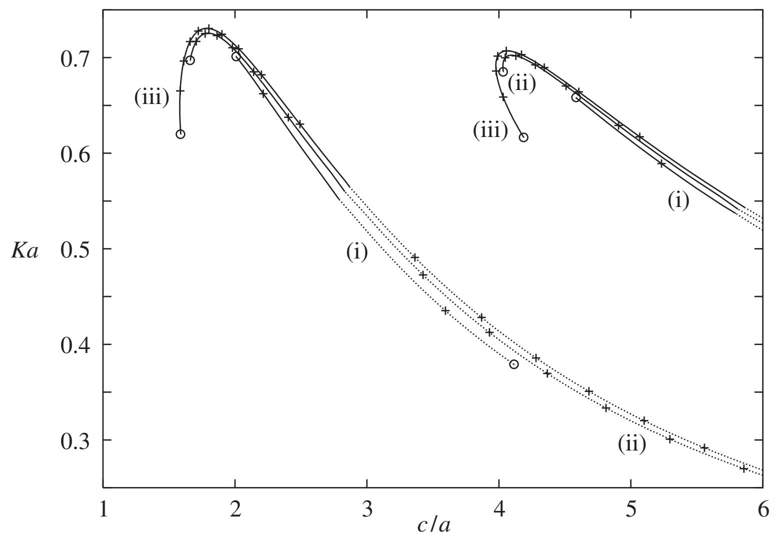

Figure 5. The locus of trapped waves in $(Ka, c/a)$ parameter space as the angle of inclination, δ, of a pair of flat plates in infinite depth for plate lengths: (i) $a/d = 5$, (ii) $a/d = 7.5$, (iii) $a/d = 10$. Points $\delta = 0°$ results are marked with open circles and intervals of 1° in δ are marked by plus signs.

5. Conclusions

The methods introduced in Porter (2002) (referred to in the text as I) for the scattering of waves by submerged cylinders has been used to investigate trapped waves above pairs of submerged cylinders. The motivation for seeking these trapped modes has come from the fact that there are a number of families of submerged obstacle for which zeros of transmission exist at particular frequencies. A wide-spacing approximation to wave trapping argues that two such obstacles, arranged symmetrically about a vertical plane and placed far enough apart, will trap a wave of this frequency between the obstacles, as the wave makes permanent reflections from each obstacle. However, small evanescent effects will always need to be included and so a full formulation of the problem is developed based on the methods in I. Trapped waves are shown to correspond to two real conditions being met simultaneously. These are shown numerically to correspond to the point at which two numerically generated curves intersect one another. The existence of trapped waves is convincing, since the existence of the crossing point is unaltered by either numerical rounding errors or the accuracy of the approximation used. The Galerkin method used in I has been adapted for the case here and equally impressive numerical results have been reported. Using this method a variety of wave-trapping configurations have been found.

Simon & Ursell (1984) showed that if submerged obstacles are contained entirely within two straight lines drawn at 45° to the vertical from a single point on the free surface, then no trapped waves could exist. In this paper we have provided examples of trapped waves supported by totally submerged obstacles. For each configuration two straight lines symmetrical about the vertical can be drawn from a point on the free surface enclosing the trapping structure for which the angle, α, of the lines with respect to the vertical is a minimum. It is interesting to see how close this angle can be made to the figure of 45° derived in Simon & Ursell (1984). Although only a limited set of results has been considered in this paper, the smallest angle beneath which the entire trapping structure can be contained is approximately $\alpha = 83.3°$, found for a symmetric pair of inclined plates of length $a/d = 10$ and inclined at an angle of $\delta = 5.7°$ to the horizontal. It is quite possible that with further experimentation, the figure of 83.3° could be reduced further.

The author thanks C. M. Linton for giving permission to reproduce his results for trapping by submerged horizontal plates.

References

Evans, D. V. & Kuznetsov, N. 1998 Trapped modes. In *Advances in fluid mechanics*, pp. 127–168. Southampton: Computational Mechanics Publications.

Evans, D. V. & Morris, C. A. N. 1972 Complementary approximations to the solution of a problem in water waves. *J. Inst. Math. Applicat.* **10**, 1–9.

Evans, D. V. & Porter, R. 1998 Trapped modes embedded in the continuous spectrum. *Q. J. Mech. Appl. Math.* **52**, 263–274.

Kuznetsov, N., McIver, P. & Linton, C. M. 2001 On uniqueness and trapped modes in the water wave problem for vertical barriers. *Wave Motion* **33**, 283–307.

Linton, C. M. & Kuznetsov, N. 1997 Non-uniqueness in two-dimensional water wave problems: numerical evidence and geometrical restrictions. *Proc. R. Soc. Lond.* A **453**, 2437–2460.

McIver, M. 1996 An example of non-uniqueness in the two-dimensional water-wave problem. *J. Fluid Mech.* **315**, 257–266.

McIver, M. 2000 Trapped modes supported by submerged obstacles. *Proc. R. Soc. Lond.* A **456**, 1851–1860.

Parsons, N. & Martin, P. 1992 Scattering of water waves by submerged plates using hypersingular integral equations. *Appl. Ocean Res.* **14**, 313–321.

Parsons, N. & Martin, P. 1994 Scattering of water waves by submerged curved plates and by surface-piercing plates. *Appl. Ocean Res.* **16**, 129–139.

Porter, R. 2002 Surface wave scattering by submerged cylinders of arbitrary cross-section. *Proc. R. Soc. Lond.* A **458**, 581–606. (Preceding paper.)

Simon, M. J. & Ursell, F. 1984 Uniqueness in linearized water-wave problems. *J. Fluid Mech.* **148**, 137–154.

Yu, Y. S. & Ursell, F. 1961 Surface waves generated by an oscillating circular cylinder on water of finite depth: theory and experiment. *J. Fluid Mech.* **11**, 529–511.